Jpn. J. Appl. Phys. Vol. 41 (2002) pp. 4851–4856
Part 1, No. 7B, July 2002

A High-Speed Atomic Force Microscope for Studying Biological Macromolecules in Action

Toshio ANDO*, Noriyuki KODERA, Daisuke MARUYAMA, Eisuke TAKAI, Kiwamu SAITO and Akitoshi TODA[1]

Department of Physics, Faculty of Science, Kanazawa University, Kakuma-machi, Kanazawa 920-1192, Japan
[1]*Olympus Co., 2951 Ishikawa-machi, Hachiohji, Tokyo 192-8507, Japan*

(Received January 11, 2002; revised manuscript received February 8, 2002; accepted for publication February 12, 2002)

The atomic force microscope (AFM) is a powerful tool for imaging biological molecules on a substrate, in solution. However, there is no effective time axis with AFM; commercially available AFMs require minutes to capture an image, but many interesting biological processes occur at a much higher rate. Hence, what we can observe using the AFM is limited to stationary molecules, or those moving very slowly. We sought to increase markedly the scan speed of the AFM, so that in the future it can be used to study the dynamic behavior of biomolecules. For this purpose, we have developed various devices optimized for high-speed scanning. Combining these devices has produced an AFM that can capture a 100 × 100 pixel image within 80 ms, thus generating a movie consisting of many successive images of a sample in aqueous solution. This is demonstrated by imaging myosin V molecules moving on mica, in solution. [DOI: 10.1143/JJAP.41.4851]

KEYWORDS: AFM, protein, biomolecules, real-time imaging, dynamics

1. Background

Protein consists of 20 kinds of amino acids. Ribosomes synthesize polypeptides by connecting these amino acids in one dimension according to the information encoded in mRNA as a sequence of four kinds of nucleotides. A polypeptide folds into a 3D structure by itself, or with the assistance of molecular chaperones. Although many possibilities may exist for the 3D structural arrangement, the resulting 3D structure is strictly unique, and only the protein having this unique 3D structure can perform its particular physiological function. Hence, the "structure" and "function" of protein are tightly related. Protein is a simple material without any mysterious enigmas. Yet, protein performs very sophisticated functions that cannot be achieved by man-made creatures. Why and how do these functions proceed? They must be understood in the framework of existing theories of chemistry and physics. The function of a protein is supported by its structure, and therefore must be understandable by knowing its structural details. Although this seems reasonable, it is a problem how to learn the structural details of protein. Is the atomic structural information of protein revealed by X-ray crystallography sufficient for understanding the mechanism? Apparently, it is not. We now have many proteins whose atomic structures are well known. Yet, we have only a small number of proteins whose functions seem to have been well clarified from their structures. Moreover, these few proteins perform only simple functions, for example, attachment to and detachment from a ligand, or catalysis of a simple reaction.

Motor proteins (such as myosin, kinesin, dynein) are very sophisticated nano-machines. They produce force to pull cytoskeletal fibers, or to move along these fibers. This mechanical function is coupled to ATP hydrolysis, and the chemical energy released by the hydrolysis is transduced to mechanical energy. In our laboratory, we have recently found that single molecules of myosin V, purified from chick brains, travel a long distance along actin filaments after association with them.[1)] To observe this movement, myosin V was labeled with a fluorophore, and the movements of the resultant fluorescent spots on the protein were recorded as video images (Fig. 1). However, from the images, we do not know how myosin V behaves dynamically during this movement. In particular, researchers who study biological molecular motors are very enthusiastic about understanding the dynamic aspects of these proteins in action. Their enthusiasm has led to the development of new techniques for studying the proteins. These techniques have also been used in other fields of biological science. However, a technique that allows direct observation of nanometer-scale dynamic behavior of individual protein molecules has long been sought. X-ray crystallography, optical and electron microscopy, and nuclear magnetic resonance (NMR) are insufficient for this purpose. The information we need in order to understand a particular protein is; (a) its physiological action such as movement of a molecular motor, (b) the fine structure of the protein with atomic resolution, (c) the kinetics of the chemical reactions involved such as ATP hydrolysis, and (d) the structural dynamics of the protein in action. The first aspect can be studied by optical microscopy, the second by X-ray crystallography, and

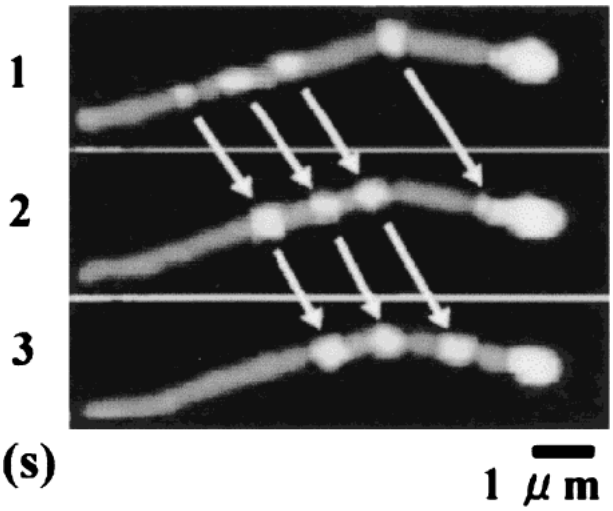

Fig. 1. The video images at 1 s intervals of processive movement of single molecules of myosin V along an actin filament. Bright spots representing individual myosin V molecules are moving up to the end of an actin filament. The end is becoming brighter because of a constant stream of myosin V traffic. The velocity of this processive movement is about 1 μm/s.

*E-mail address: tando@kenroku.kanazawa-u.ac.jp

the third can be studied by various transient techniques. The fourth aspect is the most difficult to study. The time scale of a protein's structural dynamics in action may range from a nanosecond to a second. However, the time scale of physiological action ranges from a millisecond to a second. An atomic force microscope (AFM) allows observation of protein in solution. However, its scan speed is too low to capture protein in motion. A high-speed AFM seems to be only the device able to fulfill the missing part among techniques in this physiologically intimate time scale. It is this that has been our motivation for developing a high-speed AFM capable of acquiring many successive 100^2 pixels images at intervals of 80 ms.[2)] In this report, we give brief descriptions of critical aspects of this development, and discuss the significance of this new instrument to life science.

2. Factors Limiting the Scan Speed of AFM

What factors of the AFM limit the scan speed? Here, we consider only the tapping mode of operation (Digital Instruments, Santa Barbara, CA). This is the mode most suitable for observing soft samples weakly attached to a substrate, in solution.[3)] In this mode the cantilever is oscillated at (or near) its resonance frequency. The oscillating tip briefly taps the surface of the sample at the bottom of each swing, resulting in a decrease in the oscillation amplitude. This decrease gives information of the sample height. The cantilever, therefore, has to oscillate for at least one cycle for each pixel of the image. To obtain an image consisting of $N \times N$ pixels using a cantilever having the resonance frequency of F_c, we require an imaging time (T), given by

$$T \geq 2N^2/F_c. \tag{1}$$

An imaging time of 80 ms for 100×100 pixels requires a resonance frequency higher than 250 kHz in water. When the measurement of the oscillation amplitude requires 5–6 waves of oscillation, the required resonance frequency should be 5–6 times higher than 250 kHz. It seems impossible to manufacture such cantilevers, because cantilevers useful for imaging soft samples should have a small spring constant as well, so as to minimize the tip-sample interaction force. Therefore, in addition to cantilevers having a high resonance frequency, we need an RMS-DC converter that can output the amplitude voltage of the input sinusoidal signals as quickly as possible.

In addition to the resonance frequency of cantilevers, we have to consider another factor that limits the scan speed. Suppose that a sample on a substrate has a periodicity of λ, and the sample stage is moved horizontally with a velocity of V_s, the spatial frequency of $1/\lambda$ is converted to a temporal frequency of V_s/λ. The feedback system, that keeps the cantilever's oscillation amplitude constant, moves the sample stage up and down. The feedback bandwidth (F_b) should be wider than V_s/λ. Therefore, the scan speed is limited by the bandwidth as $V_s < \lambda F_b$. This scan speed determines the imaging time as

$$T = 2pN^2/V_s \geq 2pN^2/\lambda F_b, \tag{2}$$

where p is the pixel size. For example, if $T = 80$ ms, $N = 100$, $p = 2$ nm, and $\lambda = 10$ nm, then there is a required feedback bandwidth larger than 50 kHz. Various devices are involved in the feedback loop, as shown in Fig. 2.

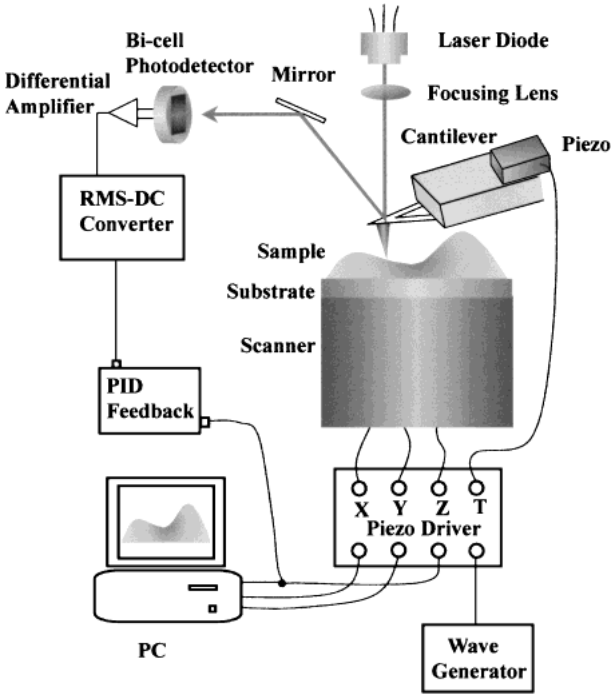

Fig. 2. A schematic of a conventional AFM system for the tapping mode of operation. The cantilever is oscillated by excitation with the electric piezo actuator. The laser beam reflected back from the cantilever is incident onto the bi-cell photodetector. The output from the differential amplifier represents the deflection of the cantilever. The output from the RMS-DC converter represents the oscillation amplitude of the cantilever. When the sample stage is scanned horizontally, the tip-sample interaction changes due to the variations of sample height, resulting in changes in the amplitude. The PID feedback circuit detects the difference between this amplitude and its preset value, and outputs a signal to the piezo driver in order to move the sample stage vertically. This is quickly repeated until the difference becomes zero. Thus, the cantilever's oscillation amplitude is kept constant during the scanning of the sample stage, and therefore, the movement of the sample stage follows the topography of the sample.

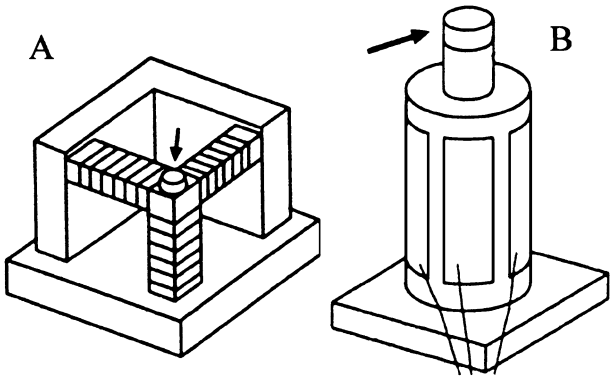

Fig. 3. Sketches of AFM scanners with conventional designs. (A) a tripod type, (B) a cylindrical type. The arrows indicate the sample stages.

It is not very difficult to achieve a high bandwidth for electronic devices. However, the scanner is the mechanical device most difficult to optimize for high-speed scanning. A well-known guiding principle for fabricating a mechanical device with a high resonance frequency is to make it with a small, compact, and light body. The sketches (Fig. 3) show the conventional designs for the scanners that have been employed for the AFM. As long as the dimensions of these scanners are sufficiently large, the movements along the three axes do

not interfere with each other. However, such large dimensions result in a low resonance frequency. We, therefore, require a different design for the high-speed scanner. Also required of the high-speed scanner is high rigidity against the impulsive forces produced by rapid movements of the piezo actuators. When an object having the mass of 1 g is moved at 50 kHz with an amplitude of 10 nm, a peak impulsive force of 1.0 N is produced. The AFM scanner should not generate unwanted vibrations of even 1 nm against this impulsive force. Therefore, the required rigidity becomes 100 kg/μm. From simple calculations, it is evident that it is impossible to fabricate a mechanical device having such a high resonance frequency as well as high rigidity. Therefore, we need alternative guidelines for fabricating a high-speed scanner. Several laboratories throughout the world have been trying to develop a high-speed AFM.[4–6] They must also have encountered the greatest difficulty when making a high-speed scanner. An alternative means of achieving a high-speed scanner is to use a cantilever with an integrated piezoelectric actuator such as zinc oxide.[7] However, such integration inevitably results in a large spring constant of the cantilever.

3. New Devices

3.1 Small cantilevers

A high resonance frequency and a small spring constant are conflicting requirements for any mechanical device. This is evident from the following equations for a strip type cantilever.

$$F_c = 0.56\frac{d}{L^2}\sqrt{\frac{E}{12\rho}}, \tag{3}$$

$$k = \frac{wd^3}{4L^3}E, \tag{4}$$

where k is the spring constant, d, L, and w are the thickness, the length and the width of the cantilever, and E and ρ are the Young's modulus and the density of material used for the cantilever, respectively.[8] These conflicting requirements can be met only by using small dimensions. We fabricated small cantilevers from silicon nitride using micromachining techniques (Fig. 4). They are 140 nm thick, 2 μm wide, and 9–11 μm long. The rear side of each cantilever is coated with gold of 20 nm thickness. All surfaces of the cantilevers are further coated with osmium, about 2 nm thick. The tips were grown by electron-beam deposition,[9] with a growth rate of about 5 nm/s. The tip length was adjusted to about 1 μm. Because in the AFM setup the cantilever is slightly tilted from the sample substrate, the tip was grown at a slightly tilted angle to make its axis approximately normal to the substrate plane. The radius of the tip end is 5–8 nm. This radius is influenced by the parameters of the scanning electron microscope (SEM, SM-520, resolution 2 nm, Topcon, Tokyo). In our experience, the shorter working distance and the smaller spot size result in a smaller tip radius. The mechanical properties of the cantilevers were tested by measuring the spectra of their thermal motions. The resonance frequencies are 1.3–1.8 MHz in air, and 450–650 kHz in water, and the spring constants are estimated to be 150–280 pN/nm. The highest resonance frequency in water, i.e., 650 kHz, can reduce the imaging time to 30 ms for 100 $\times$ 100 pixels.

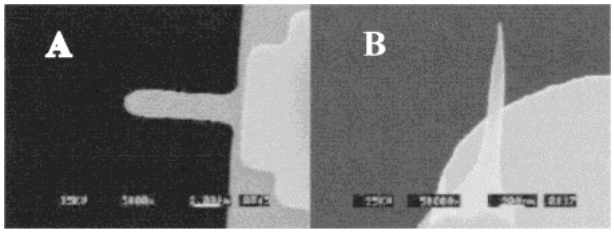

Fig. 4. Electron micrographs of the small cantilever developed for our high-speed AFM. (A) the cantilever made from silicon nitride has no tip. (B): a tip was grown on the cantilever end by electron-beam deposition.

3.2 RMS-DC converter

Conventional RMS-DC converters require at least 5–6 waves for conversion. This requirement arises because the converter has to use a low-pass filter in order to separate the carrier (basic) wave from the amplitude-modulation wave. We designed a new converter that requires only a half wave for conversion (Fig. 3 of ref. 2). This converter is a type of peak-hold circuit. Two S/H circuits hold the peak and bottom voltages separately. The timing signals for this holding are made by the input sinusoidal signal itself. This guarantees stable and precise conversion even when the cantilever oscillation changes its frequency and phase. The phase of the AC input signal is shifted by 90°, so its output signal crosses zero voltage when the input signal reaches the peak or bottom. The zero-cross comparators generate rectangular wave signals at this time. The difference between the two voltages held with the two S/Hs is output as the amplitude (not the RMS value) of the input sinusoidal signal. This new converter is satisfactory for an input sinusoidal signal of up to 1 MHz.

3.3 Optical deflection detection system

Since the cantilevers are very small, we required that the laser beam be focused onto the small cantilever as a small spot. Therefore, we could not use the optical deflection detection system that has widely been used in commercial AFMs. We designed an objective-lens type of deflection detection system (Fig. 5). The incident laser beam is focused onto

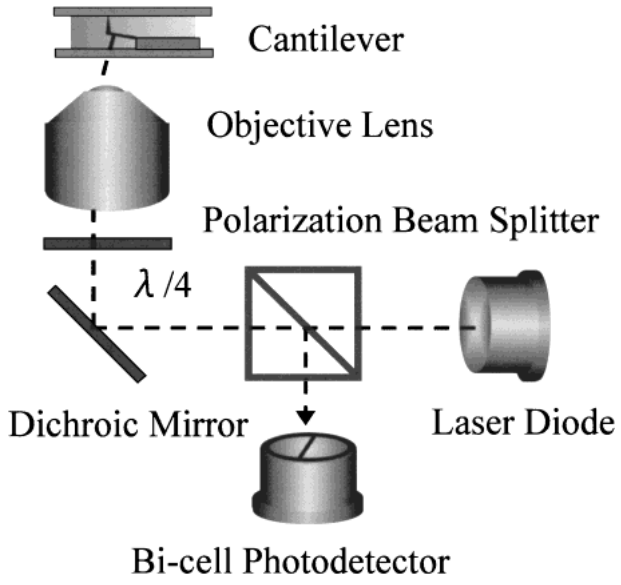

Fig. 5. A schematic of the objective-lens type of optical deflection detection system. For details, see the text.

a small cantilever using an objective lens (CFI Plan Fluor ELWD 20 × C, Nikon). The reflected beam is collected and collimated with the same objective lens. The incident and reflected beams are separated by a polarization beam splitter and a quarter-wavelength plate. The incident beam is entered into the objective lens at a slightly off-centered position to make the outgoing beam axis normal to the plane of the cantilever. The focused spot is 2–3 μm in diameter, sufficiently small for our small cantilevers. The optical lever magnification is about 2,000. This large magnification results from the short length of the cantilevers.

3.4 Scanner

As mentioned above, it is impossible to fabricate a mechanical device with the high resonance frequency (> 50 kHz) and high rigidity (> 100 kg/μm) required of the high-speed scanner. We considered the following possibility: (1) We might somehow reduce the resonance amplitude even when the resonance occurs at low frequencies; (2) We might somehow counteract the impulsive forces produced by the quick movement of the piezo actuators. After making and testing a number of scanners with different designs, we reached the design illustrated in Fig. 6 (also in Fig. 2 of ref. 2). Stack-type piezoelectric actuators (AE0203D04, Tokin, Tokyo) are used in this scanner. They have a resonance frequency of 260 kHz in free oscillation, their maximum displacement is 4.5 μm, and their capacitance is 90 nF. This scanner has a two-layered structure. One layer is for scanning in the *y*-direction, and the other layer is for scanning in the *x*- and *z*-directions. This structure guarantees no interference between the movements along the three axes. The *z*-scanner has two *z*-piezo actuators placed in opposite directions to one another. A sample stage is attached to one of the *z*-piezo actuators via a thin layer of vacuum grease. These actuators are displaced simultaneously in the same distance, but in counter directions, so that any impulsive forces produced are canceled out. The base plate (Base-2), to which the two *z*-actuators as well as an *x*-actuator are attached, is clamped in the *z*-direction by two flat surfaces (Base-1 and Plate-2) via steel ball bearings. This design allows smooth movement of the base (and hence, the sample stage) in the *x*-direction, and minimizes the vibrations of the base in the *z*-direction. When the *z*-piezo is displaced quickly, hydrodynamic force is generated as a reaction from the sample solution to the sample stage (Fig. 7). To minimize this reactive force, a glass of circular-trapezoid shape with a small top surface of 1 mm diameter is used as the sample stage. A result of the performance test of the *z*-scanner is shown in Fig. 8. In the setup shown in Fig. 8, the oscillation amplitude of the sample stage was measured as a function of the driving frequency. The oscillation amplitude was constant up to about 60 kHz. The large amplitude observed at 100 kHz is due to the resonance of the piezo actuators themselves (when one end of a piezo actuator is fixed, its resonance frequency becomes half the resonance frequency of that when it is oscillated with both ends free). Because the devices involved in the feedback loop, other than the scanner, have bandwidths much wider than 60 kHz, the feedback bandwidth is thus determined to be about 60 kHz. To confirm this conclusion, we took a pseudo-image by oscillating the sample stage at 55 kHz and with the amplitude of 20 nm using a piezo film, without scanning in the *x*- or *y*-direction. The imaging time was 40 ms for 100 × 100 pixels. As shown in Fig. 9, the periodical pattern of 55 kHz was successfully imaged.

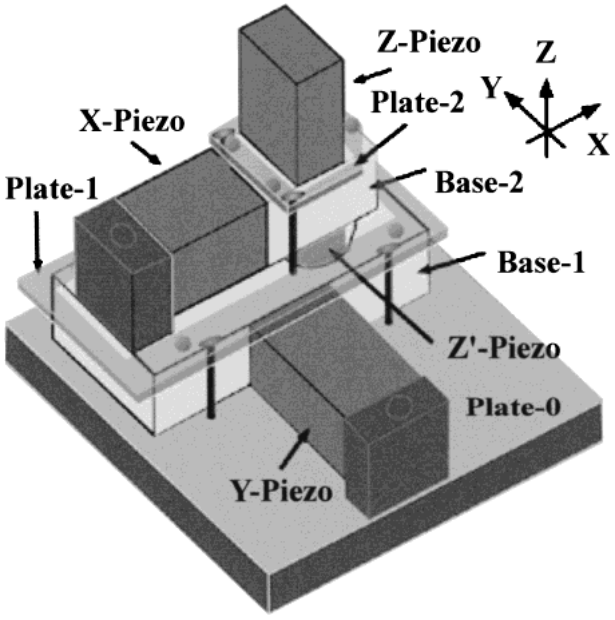

Fig. 6. Scanner assembly. The piezo actuators are 5 mm long, 4 mm wide, and 2.7 mm thick. Base-2 ($6 \times 6.7 \times 2.7$ mm^3) is clamped in the *z*-direction between Plate-2 and Base-1 via six steel ball bearings (three for the top, and the other three for the bottom). Base-1 ($10 \times 16.7 \times 2.7$ mm^3) is also clamped in the *z*-direction between Plate-1 and Plate-0 via six steel ball bearings (three for the top, and the other three for the bottom). The bearings are 1 mm in diameter. Each clamp is made using three screws placed close to each of the ball bearings. A sample stage is attached to the top of the *z*-piezo.

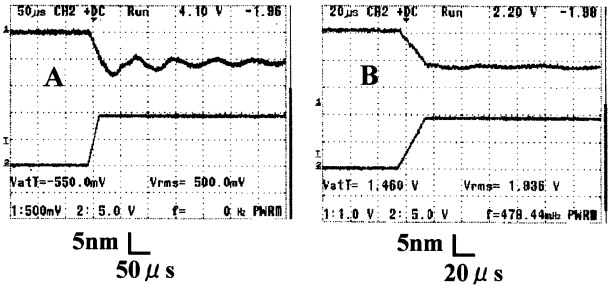

Fig. 7. Dependence on the shape of the sample stage of the cantilever's response when the sample stage is quickly moved toward the cantilever. The lower signals represent the voltage applied to the *z*-actuator to move the sample stage. The upper signals represent the cantilever deflection. The time and length scales are shown under each panel. The tip of the cantilever in water is kept in contact with a mica surface. (A) the sample stage is a slide glass cut to 5 × 5 mm square. (B) the sample stage is a glass of circular-trapezoid shape with a small top surface of 1 mm diameter. When this test is carried out with the cantilever being oscillated, its amplitude does not vibrate so significantly as seen in (A), irrespective of the shape of the sample stage.

4. Imaging

Prior to reaching the final phase of this development of a high-speed AFM, the minimum time for taking an image with 100 × 100 pixels was limited to ≥ 0.4 s. This limitation was due to overload in the PC processing such as data sampling and the signal generation for the *x*- and *y*-scans. With this imaging time, we could not clearly snap an image of myosin

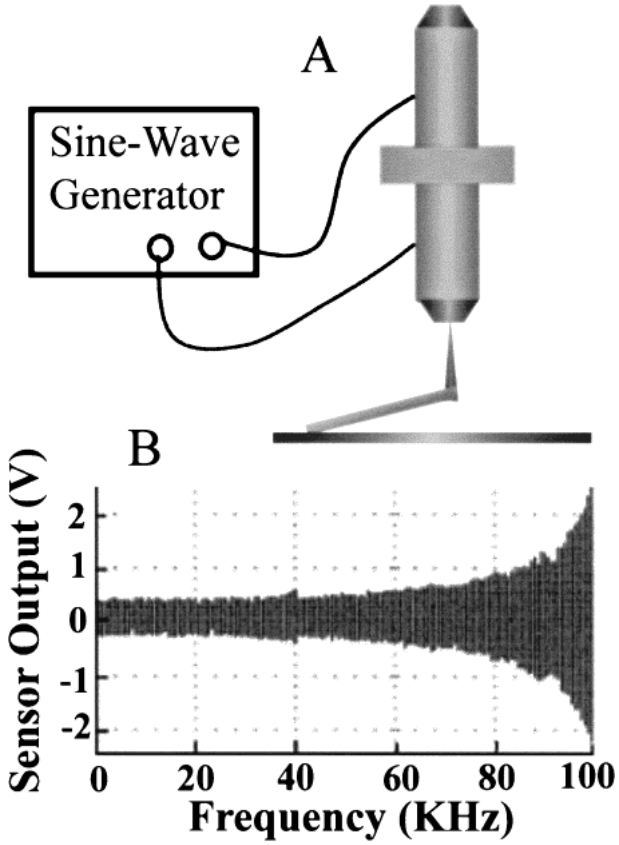

Fig. 8. Performance test of the high-speed *z*-scanner. (A) the experimental setup for this test. The cantilever tip immersed in water is kept in contact with the sample stage. The frequency for driving the *z*-actuators is scanned from 1 kHz to 100 kHz. (B) the oscillation of the sample stage as a function of the driving frequency. The oscillation is measured by detecting the cantilever deflection.

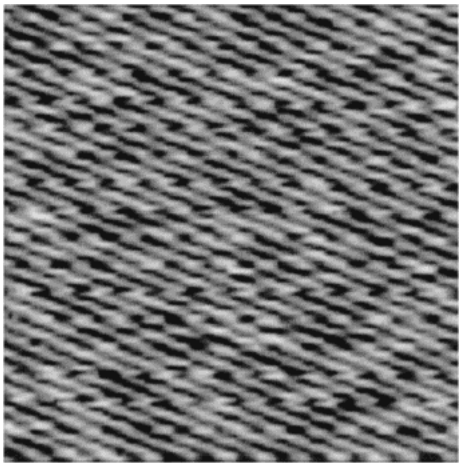

Fig. 9. A pseudo-image obtained with a film piezo attached to the sample stage being oscillated at 55 kHz, without scanning in the *x*- or *y*-direction.

V weakly attached to a mica surface, in solution. This implies that myosin V might be rapidly moving on the substrate, in solution. Therefore, we imaged dust firmly attached to a mica surface, in solution, and made a movie by zooming-in and zooming-out (changing the scan size between 600 nm and 2500 nm) (Fig. 10). In observing the successive images we noticed that mirror images appeared at the left margin of the images. This is caused by the inertia of the mass attached to

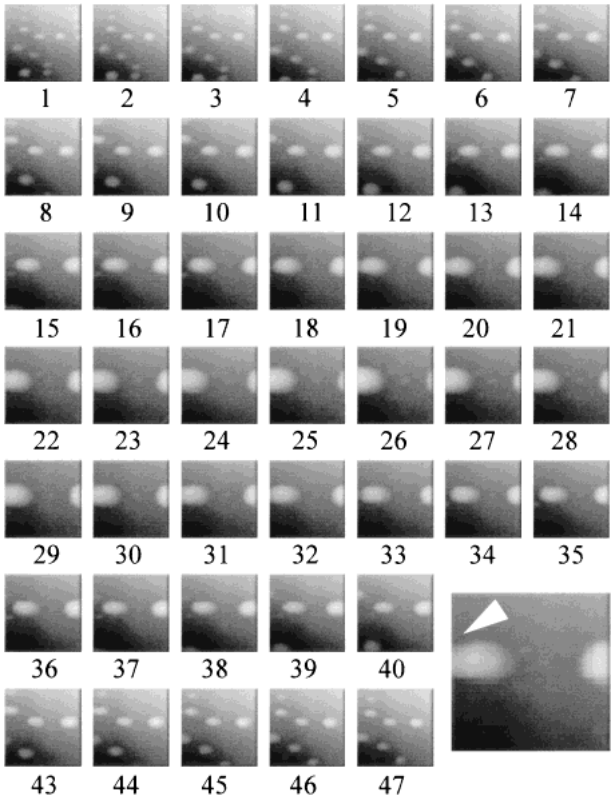

Fig. 10. Successive images, at 0.4 s intervals, of dust attached to a mica surface, in water. The size of the scan area is changed every 0.4 s by zooming in and out on the sample. The numbers shown under each image are the frame numbers. The magnified image in the lower right corner is of the 21st image, and a mirror image appearing is indicated by an arrow head.

the free end of the *x*-piezo. Therefore, the mass was reduced slightly. Moreover, to avoid the overload of the PC processing, we designed a circuit that generates signals for *x*- and *y*-scans. Thus, the PC can concentrate on data sampling. According to eqs. (1) and (2), the feedback bandwidth of 60 kHz as well as the high resonance frequencies of the small cantilevers can reduce the time for capturing an image with 100^2 2 nm pixels to 70 ms, as long as the apparent width of the sample is not too small. We examined whether imaging can really be carried out at (or near) the maximum rate predicted here. Myosin V directly attached to mica, in solution, was imaged successively (240 nm scan range; 100^2 pixels) for 4 s (50 frames). The scan rate was 1.25 kHz, corresponding to a tip speed of 0.6 mm/s, and the frame rate was 12.5/s. The angle between the head and neck regions dramatically changed (Fig. 11; Fig. 5 of ref. 2). The reconstructed movie is available from the CD-ROM of "Molecular Biology of The Cell", 4th ed. (Garland Science Publishing, 2002).

5. Significance of the High-Speed AFM to Life Science

In life science, it has been a dream to view the nanometer-scale dynamic behavior of individual biopolymers in solution. The capacity to acquire successive images every 80 ms will allow a large expansion in the scope of biological processes that can be examined in real time. In the near future, we should be able to observe the behavior of processive motors such as kinesin[10] and myosin V[1] moving along their tracks, of molecular chaperones assisting a polypeptide chain

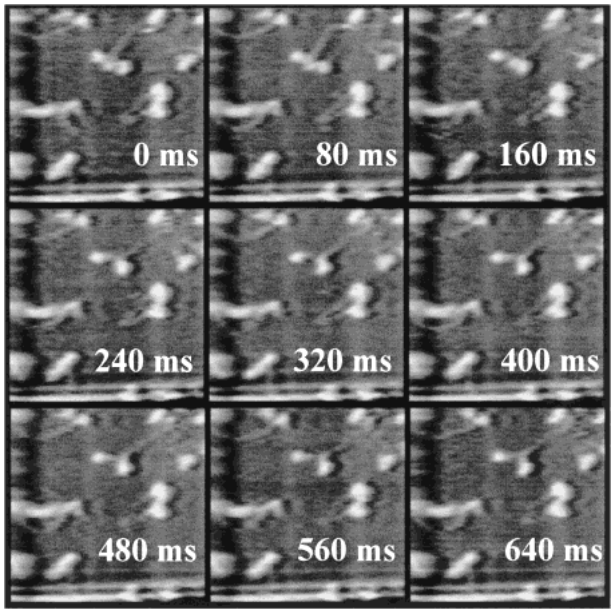

Fig. 11. Successive images of myosin V on mica, in buffer solution. The same area of $240 \times 240\,nm^2$ was imaged 50 times with 100×100 pixels. Only nine successive images are shown. The reconstructed movie is available from the CD-ROM of "Molecular Biology of The Cell", 4th ed. (Garland Science Publishing, 2002).

to fold, or of a ribosome synthesizing a polypeptide according to the nucleotides sequence on mRNA. Such direct observations will provide insight into the mechanisms by which biomolecular machines operate. We think that the high-speed AFM has further potential in life science. If we can link dynamic images of a protein acquired by the high-speed AFM to its known atomic structure, we may be able to construct dynamic atomic models not obtainable by other techniques. How can we make such a link? The AFM can view only the surface of the protein, from one side. The other side, facing the substrate, cannot be observed. Therefore, the information obtained by using the AFM seems too remote from the atomic structure of the protein. Therefore, we may require additional structural information that can mediate this linking process. Cryo electron microscopy (cryo-EM) can view the inside of a protein, and report an electron density map of lower resolution than is achievable with X-ray crystallography. Fitting of cryo-EM images of protein to the corresponding atomic structure has already been carried out successfully in several cases. Suppose cryo-EM images are obtained for protein molecules that were performing a function immediately before freezing; these molecules will be found with different conformations among these images. These conformations must occur on a single molecule of protein that dynamically changes its structure along the time axis. Therefore, the conformations found in the cryo-EM images can be aligned along the time axis, reflecting the dynamic AFM images. Then, we must deform the atomic structure so as to fit it to the conformations found in the cryo-EM images. In this way, we can construct dynamic atomic models that move and thus reflect the AFM movies. By analyzing such a model (for example, by calculating the potential energies of the atomic structures aligned along the time axis), we can probably understand the physics of its physiological function from the structural details. The static atomic structures of many proteins have been revealed by X-ray crystallography. However, the basic framework of structural biology has not been changed significantly since the first success by Professor Perutz in 1936. We hope that the high-speed AFM will enable a breakthrough in structural biology in the future.

Acknowledgement

This work was supported by the Proposal-based New Industry Creative Type Technology R&D Promotion Program from the New Energy and Industrial Technology Development Organization (NEDO) of Japan to T.A.

1) T. Sakamoto, I. Amitani, E. Yokota and T. Ando: Biochem. Biophys. Res. Commun. **272** (2000) 586.
2) T. Ando, N. Kodera, E. Takai, D. Maruyama, K. Saito and A. Toda: Proc. Natl. Acad. Sci. USA **98** (2001) 12468.
3) C. A. J. Putman, K. O. Van der Werf, B. G. De Grooth, N. F. Van Hulst and J. Greve: Appl. Phys. Lett. **64** (1994) 2454.
4) M. B. Viani, T. E. Schäffer, G. T. Paloczi, L. L. Pietrasanta, B. L. Smith, J. B. Thompson, M. Richter, M. Rief, H. E. Gaub and K. W. Plaxco: Rev. Sci. Instrum. **70** (1999) 4300.
5) T. Sulcheck, R. Hsieh, J. D. Adams, S. C. Minne, C. F. Quate and D. M. Adderton: Rev. Sci. Instrum. **71** (2000) 2097.
6) S. J. T. van Noort, K. O. van der Werf, B. G. de Grooth and J. Greve: Biophys J. **77** (1999) 2295.
7) S. C. Minne, S. R. Manalis and C. F. Quate: Appl. Phys. Lett. **67** (1995) 3918.
8) D. Sarid: *Scanning Force Microscopy with Applications to Electric, Magnetic, and Atomic Forces* (Oxford Univ. Press, New York, 1991) Chap. 1.
9) D. J. Keller and C. Chih-Chung: Surf. Sci. **268b** (1992) 333.
10) R. D. Vale, T. Funatsu, D. W. Pierce, L. Romberg, Y. Harada and T. Yanagida: Nature **380** (1996) 451.